

# Shape-Shifting Micro- and Nanopatterns Controlled by Temperature

Christopher M. Kolodziej and Heather D. Maynard\*

Department of Chemistry and Biochemistry and the California NanoSystems Institute, University of California, Los Angeles, 607 Charles E. Young Drive South, Los Angeles, California 90095, United States

**S** Supporting Information

**ABSTRACT:** Herein, features that alter their shape to form a different pattern upon an external trigger are described. Electron-beam lithography was used to fabricate micrometer- and nanometer-sized surface immobilized poly(triethylene glycol methacrylate) (pTEGMA) that exhibits significant thermal responsiveness; the resulting hydrogels collapsed by up to 95% of their height upon addition of heat. Multicomponent features composed of both the thermoresponsive polymer and nonresponsive poly(ethylene glycol) (PEG) were then prepared. Upon increase in temperature, only the thermally responsive component of the pattern collapsed, causing a significant and predictable alteration in the overall pattern. Reversible micrometer- and nanometer-sized square-to-triangles, squares-to-checkerboards, smiles-to-neutral face, and zeros-to-ones shapes were shown.

There is tremendous interest in materials that reversibly alter their properties depending on the environment. For example, shape-memory materials respond to a stimulus to undergo a significant physical deformation to a predetermined shape.<sup>1–6</sup> Adaptive hydrogels, often inspired by nature, undergo significant mechanical changes to alter viscosity or modulus in the presence of a trigger.<sup>7,8</sup> Actuating materials exhibit large displacements in structure, typically involving large forces, induced by an environmental change.<sup>9–11</sup> Microorigami is a term used to describe materials that fold into three-dimensional objects upon exposure to a stimulus.<sup>12–16</sup> Often these smart/intelligent systems are reversible, and stimuli include heat, light, electricity, magnet, or binding of a (bio)molecule.<sup>9,10,17–19</sup> These hydrogel materials are candidates for a myriad of exciting applications including sensors, diagnostics, coatings, miniature devices, lab-on-a-chip designs, drug delivery vehicles, and nanomachines.<sup>20,21</sup>

With the advent of micro- and nanotechnology fabrication approaches, patterned switchable surfaces are possible.<sup>22</sup> Responsive micropatterns have been prepared, and some interesting shapes have been made.<sup>23–26</sup> Switchable nanostructures have been fabricated that either actuate or deform directionally to produce interesting patterns and to control fluid flow.<sup>11,27–30</sup> Features that respond to a variety of different stimuli to reversibly swell have been exploited for applications as diverse as microfluidic valves and surfaces that manipulate and probe cells.<sup>23,26,31–33</sup> There have been exciting examples of patterns that actuate in a certain direction or materials that fold or close.<sup>11–16,27–30</sup> Yet producing arbitrary shapes that reversibly change pattern remains a significant challenge.

There are several examples of surfaces that hide or reveal words or patterns upon an external trigger.<sup>34–37</sup> Herein, for the first time we describe a straightforward approach that exploits electron beam (e-beam) lithography to produce patterns that reversibly change shape upon addition of heat.

We designed a system whereby patterns composed of contiguous thermally responsive and nonresponsive hydrogels were produced such that when the temperature is raised, the responsive component collapses causing a change in the overall shape. Polymers with side-chain oligoethylene glycol units that are thermoresponsive were utilized.<sup>38,39</sup> The lower critical solution temperature (LCST) of these polymers, where in water the polymers go through a phase transition and become insoluble and collapse, can be finely tuned by altering the polymer structure.<sup>40</sup> When attached to a surface, the thermal responsivity is retained.<sup>27,41,42</sup> In this study, micro- and nanopatterns containing regions of thermally responsive pTEGMA and regions of nonresponsive star PEG were produced by e-beam lithography. This fabrication technique allows for arbitrary pattern formation at both the micrometer and nanometer scale.<sup>43</sup> E-beam radiation readily causes PEG-based polymers to cross-link to both silicon surfaces and polymer films,<sup>43,44</sup> forming hydrogels via a radical mechanism.<sup>45</sup> The resulting hydrogels are stable on surfaces for long time periods, and thermal and photoresponsive patterns have been prepared by e-beam lithography.<sup>46,47</sup> Importantly for this study, although it is a serial technique, the alignment capability for e-beam lithography is high, allowing two different polymers to be patterned touching each other.

Thermal actuation of pTEGMA hydrogels prepared by e-beam lithography was confirmed on micro- and nanopatterned surfaces prior to preparing multicomponent patterns (Figure 1). pTEGMA was synthesized by conventional radical polymerization (number-average molecular weight ( $M_n$ ) of 22 000 Da; polydispersity index (PDI) of 2.10; LCST of 52 °C, see Supporting Information (SI) for synthesis, characterization, and confirmation of thermoresponsivity of bulk hydrogels). Dilute solutions of the polymer were then spin-coated onto silicon wafers and patterned by e-beam lithography into arrays of 5  $\mu\text{m}$  circles (Figure 1 a,b). The micropatterned substrates were mounted on top of a Peltier heater and imaged by atomic force microscopy (AFM) in water at both 22 and 65 °C (Figure 1b,c). The hydrogels had an average maximum height of 553  $\pm$  64 nm at 22 °C (Figure 1d,g) and collapsed when heated to 65 °C to an average maximum height of 29  $\pm$  6 nm (Figure 1e,h). This represents a 95  $\pm$  1% reduction in swelling. Upon cooling

Received: May 18, 2012

Published: July 17, 2012

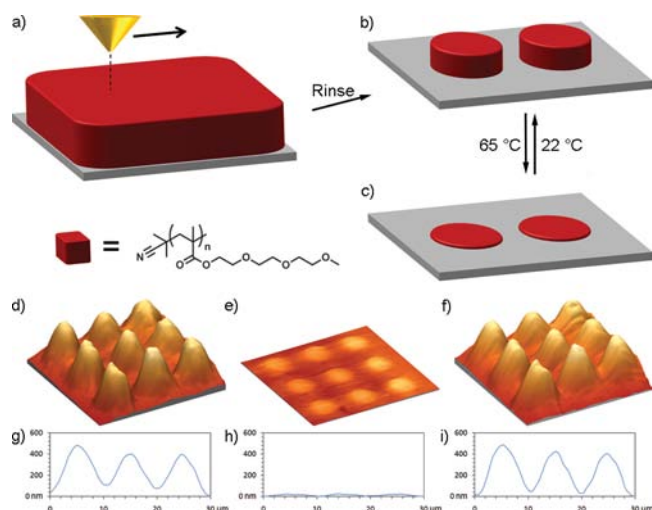


**Figure 1.** Patterning and actuation of pTEGMA hydrogels. pTEGMA film that was spin-coated on a silicon wafer is patterned by e-beam lithography (a). The uncross-linked polymer is rinsed away to reveal the discrete hydrogels (b). Upon heating to 65 °C, the hydrogels expel water and actuate vertically (c). AFM images of pTEGMA micropatterned hydrogels at 22 °C (d,g) and at 65 °C (e,h) show a dramatic decrease in height as the pTEGMA actuates. Following cooling to 22 °C (f,i), the pTEGMA microgels regain their initial height. Features 5  $\mu\text{m}$  in diameter.

to 22 °C in water, the pTEGMA hydrogels regained their initial height, with an average maximum height of  $559 \pm 64$  nm (Figure 1f,i). This demonstrates that the phase change is reversible. Likewise, nanopatterns were thermally responsive and collapsed by  $79 \pm 5\%$  (see SI, Figure S8). The overall percent change is less than for the microgels; however, this is likely due to limitations in the accuracy of the height measurement of the small features. Micron-sized hydrogels of the nonresponsive eight-arm PEG polymer hydrogels were also fabricated. Upon increase in temperature, the height change was approximately  $20\% \pm 14\%$  (see SI, Figure S7). This value is significantly less than the pTEGMA gels and, with the error of the measurement, not statistically significant. Thus, the eight-arm PEG could be utilized as a relatively nonresponsive component.

Micropatterns that contained both eight-arm PEG and pTEGMA were made in order to investigate changing the shape of a surface feature in a predictable manner with temperature. Two different sets of shapes were investigated: square features that change to triangles and a solid block that changes to a checkerboard pattern as the temperature is increased (Figure 2). The square-to-triangle multicomponent patterns were created by first spin-coating silicon wafers containing prefabricated gold electrodes for use as alignment marks with a 0.38% w/v solution of 8-arm PEG. This concentration was determined experimentally to produce a film of the same height as the 1% w/v solution of pTEGMA (see SI, Figure S6). The final relative heights of the surface features typically do not correspond exactly to relative original film heights, likely due to differences in polymer structure and required dosage to cross-link; yet, uniform relative film heights do result in more uniform multicomponent features. E-beam lithography was then used to write  $5 \times 5 \mu\text{m}$  isosceles triangles composed of 8-arm PEG. The substrates were rinsed to remove the uncross-linked 8-arm PEG, and then spin-coated with a 1% w/v solution of pTEGMA. Two  $2.5 \times 5 \mu\text{m}$  right triangles were

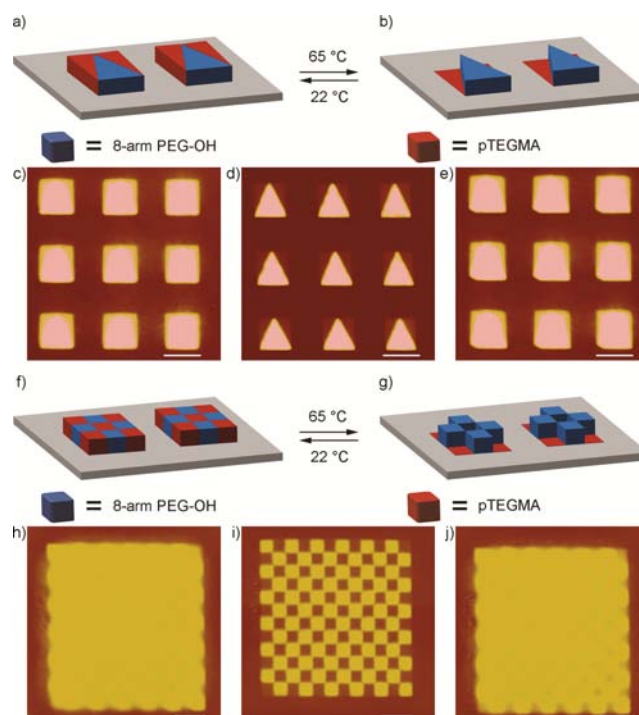


**Figure 2.** Micropatterned shape-shifting pTEGMA/eight-arm PEG patterns. AFM imaging of square-to-triangle pTEGMA/PEG micropatterns show square hydrogels at 22 °C (a,c). Upon heating to 65 °C the pTEGMA regions collapse revealing triangular 8-arm PEG hydrogels (b,d). Following cooling back to 22 °C the pTEGMA regions reswell, and the hydrogels again become squares (a,e). AFM imaging of block-to-checkerboard pTEGMA/8-arm PEG micropatterns shows a single hydrogel block at 22 °C (f,h). Upon heating to 65 °C the pTEGMA regions collapse revealing a checkerboard pattern of 8-arm PEG hydrogels (g,i). Following cooling back to 22 °C the pTEGMA regions reswell, and the hydrogel again becomes a continuous block (f,j). Scale bars = 5  $\mu\text{m}$ .

then patterned in the pTEGMA film around each 8-arm PEG feature to produce a contiguous square-shaped feature (Figure 2a). AFM images of the pTEGMA/8-arm PEG micropatterns in water at 22 °C showed uniform square features (Figure 2c). Upon heating to 65 °C, the pTEGMA portions of the patterns expelled water and collapsed to  $21 \pm 1\%$  of their initial height (from  $162 \pm 14$  to  $34 \pm 5$  nm), while the 8-arm PEG portions remained hydrated to a greater degree, at  $73 \pm 4\%$  of their initial height (from  $236 \pm 22$  to  $172 \pm 17$  nm), thus appearing as triangles (Figure 2b,d). When the patterns were again cooled to 22 °C, the pTEGMA portions rehydrated, regaining their initial heights ( $165 \pm 11$  nm) and returning the shapes of the features to squares (Figure 2e). In a similar fashion, squares that changed to checkerboards were fabricated (Figure 2f–j), and the height changes upon heating are summarized in the SI. The heating and cooling cycles were repeated for each of the above, and it was found that after the second and third cycles, respectively, the thermally responsive polymer lost approximately 20% of its original height (see SI, Figure S9). The origin of this is not known and may be due to hydrolysis of the polymer side chains. Still the features are fully reversible for at least one cycle.

E-beam lithography is capable of high resolution,<sup>48</sup> and multicomponent nanoscale features are readily accessed. To test this, actuating smiley faces and nanopatterns that convert between zeroes and ones were fabricated (Figure 3). First, four

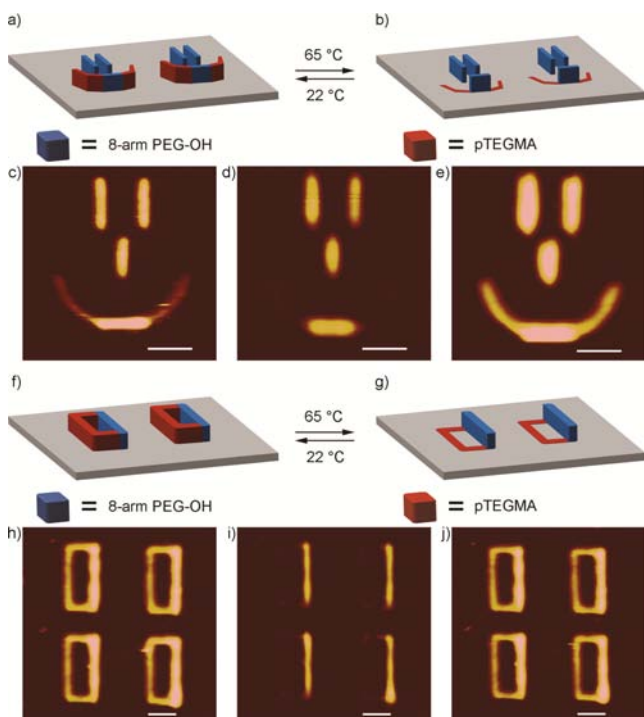


**Figure 3.** Nanopatterned shape-shifting pTEGMA/8-arm PEG hydrogels. AFM imaging of a smiley-face pTEGMA/8-arm PEG nanopattern shows the smiley-face at 22 °C (a,c). Upon heating to 65 °C the pTEGMA regions collapse removing the “smile” (b,d). Following cooling back to 22 °C the pTEGMA regions reswell, and the hydrogels again form a smiley-face (a,e). AFM imaging zero-to-one pTEGMA/8-arm PEG nanopatterns show hydrogel zeroes at 22 °C (f,h). Upon heating to 65 °C the pTEGMA regions collapse revealing 8-arm PEG hydrogels in the shape of ones (g,i). Following cooling back to 22 °C the pTEGMA regions reswell, and the hydrogels again become zeroes (f,j). Scale bars = 1  $\mu\text{m}$ .

lines composed of eight-arm PEG were written on silicon wafers in the shape of a face. pTEGMA lines were then added to form a smiley face (Figure 3a). AFM images of the nanopatterned hydrogels at 22 °C in water showed the pattern (Figure 3c). Upon heating to 65 °C, the pTEGMA portions of the pattern collapsed to  $48 \pm 5\%$  of their initial height (from  $42 \pm 2$  to  $20 \pm 2$  nm), while the 8-arm PEG portions remained hydrated to a greater degree, at  $87 \pm 3\%$  of their initial height (from  $62 \pm 2$  to  $54 \pm 3$  nm), removing the “smile” (Figure 3b,d). Cooling back to 22 °C restored the smiley face (Figure 3e). The pTEGMA portions rehydrated to their initial height ( $40 \pm 2$  nm). Multicomponent nanopatterns that convert between representations of zeroes and ones were also created. First, lines composed of eight-arm PEG were written on silicon wafers followed by three pTEGMA lines to complete the shape of the zero (Figure 3f). AFM images of the pTEGMA/8-arm PEG in water at 22 °C showed an array of zeroes (Figure 3h). When heated to 65 °C, the pTEGMA portions of the pattern collapsed to  $48 \pm 5\%$  of their initial height (from  $56 \pm 1$  to  $27 \pm 2$  nm), while the 8-arm PEG portions remained hydrated to a greater degree, at  $81 \pm 3\%$  of their initial height (from  $82 \pm 2$  to  $66 \pm 2$  nm), displaying an array of ones (Figure 3g,i). Upon cooling back to 22 °C, the pTEGMA portions of the nanopatterns rehydrated and swelled to  $60 \pm 1$  nm, returning the features to the shapes of zeroes (Figure 3j). Interestingly, after the full heating and cooling cycle, the height of the pTEGMA portions of the hydrogel was slightly greater than

when initially patterned. This may be due to a more loosely cross-linked structure following partial hydrolysis of TEG side chains during the heating/cooling cycle or removal of uncross-linked polymer during the first cycle.

Collectively, the results demonstrate that micrometer- and nanometer-sized shape-shifting patterns can be achieved. Micron-sized squares-to-triangles and squares-to-checkerboards and nanosized smiles-to-neutral faces and zeroes-to-ones were demonstrated. Yet, e-beam lithography forms arbitrary shapes, and this technique should be readily translated to a large number of different forms. Thus, many different applications, such as encryption and miniature substrates for spatial and temporal cell manipulation, can be envisioned. The latter should be possible, particularly since the LCST of the patterned polymer is readily altered in a predictable manner to physiologically relevant temperatures.<sup>40</sup> The features were fabricated of thermally responsive and nonresponsive PEG polymers by sequentially exposing films to e-beam radiation. Upon increase in temperature, only the pTEGMA portions of the features collapsed. This caused a predictable and reversible change in overall pattern in both micrometer- and nanometer-sized features. Because e-beam lithography can be used to cross-link many different polymers onto the same surface,<sup>43</sup> features containing regions with different LCSTs should be possible. This could lead to shapes that change several times and morph as the temperature is increased. Patterns that respond to a variety of different stimuli, such as pH or light, should also be possible.

## ■ ASSOCIATED CONTENT

### 📄 Supporting Information

Experimental procedures, <sup>1</sup>H NMR spectra, bulk hydrogel characterization, nanoactuation, thermal cycling. This material is available free of charge via the Internet at <http://pubs.acs.org>.

## ■ AUTHOR INFORMATION

### Corresponding Author

maynard@chem.ucla.edu

### Notes

The authors declare no competing financial interest.

## ■ ACKNOWLEDGMENTS

Funding was provided by the National Science Foundation (CAREER CHE-0645793). The authors thank Adam Stieg for helpful discussions on AFM measurements. We acknowledge the use of the Scanning Probe Microscopy facility at the Nano and Pico Characterization Laboratory at the California NanoSystems Institute.

## ■ REFERENCES

- (1) Leng, J.; Lan, X.; Liu, Y.; Du, S. *Prog. Mater. Sci.* **2011**, *56*, 1077–1135.
- (2) Behl, M.; Razaq, M. Y.; Lendlein, A. *Adv. Mater.* **2010**, *22*, 3388–3410.
- (3) Osada, Y.; Matsuda, A. *Nature* **1995**, *376*, 219–219.
- (4) Lendlein, A.; Langer, R. *Science* **2002**, *296*, 1673–1676.
- (5) Lendlein, A.; Jiang, H. Y.; Junger, O.; Langer, R. *Nature* **2005**, *434*, 879–882.
- (6) Kainuma, R.; Imano, Y.; Ito, W.; Sutou, Y.; Morito, H.; Okamoto, S.; Kitakami, O.; Oikawa, K.; Fujita, A.; Kanomata, T.; Ishida, K. *Nature* **2006**, *439*, 957–960.
- (7) Shanmuganathan, K.; Capadona, J. R.; Rowan, S. J.; Weder, C. *Prog. Polym. Sci.* **2010**, *35*, 212–222.



- (8) Capadونا, J. R.; Shanmuganathan, K.; Tyler, D. J.; Rowan, S. J.; Weder, C. *Science* **2008**, *319*, 1370–1374.
- (9) Alarcon, C. d. I. H.; Pennadam, S.; Alexander, C. *Chem. Soc. Rev.* **2005**, *34*, 276–285.
- (10) Ahn, S. K.; Kasi, R. M.; Kim, S. C.; Sharma, N.; Zhou, Y. X. *Soft Matter* **2008**, *4*, 1151–1157.
- (11) Sidorenko, A.; Krupenkin, T.; Taylor, A.; Fratzl, P.; Aizenberg, J. *Science* **2007**, *315*, 487–490.
- (12) Ionov, L. *Soft Matter* **2011**, *7*, 6786–6791.
- (13) Rothmund, P. W. K. *Nature* **2006**, *440*, 297–302.
- (14) Leong, T. G.; Randall, C. L.; Benson, B. R.; Zarafshar, A. M.; Gracias, D. H. *Lab Chip* **2008**, *8*, 1621–1624.
- (15) Randhawa, J. S.; Keung, M. D.; Tyagi, P.; Gracias, D. H. *Adv. Mater.* **2010**, *22*, 407–410.
- (16) Stoychev, G.; Puretskiy, N.; Ionov, L. *Soft Matter* **2011**, *7*, 3277–3279.
- (17) Mendes, P. M. *Chem. Soc. Rev.* **2008**, *37*, 2512–2529.
- (18) Lahann, J.; Mitragotri, S.; Tran, T. N.; Kaido, H.; Sundaram, J.; Choi, I. S.; Hoffer, S.; Somorjai, G. A.; Langer, R. *Science* **2003**, *299*, 371–374.
- (19) Ehrick, J. D.; Deo, S. K.; Browning, T. W.; Bachas, L. G.; Madou, M. J.; Daunert, S. *Nat. Mater.* **2005**, *4*, 298–302.
- (20) Bath, J.; Turberfield, A. J. *Nat. Nanotechnol.* **2007**, *2*, 275–284.
- (21) Stuart, M. A. C.; Huck, W. T. S.; Genzer, J.; Mueller, M.; Ober, C.; Stamm, M.; Sukhorukov, G. B.; Szleifer, I.; Tsukruk, V. V.; Urban, M.; Winnik, F.; Zauscher, S.; Luzinov, I.; Minko, S. *Nat. Mater.* **2010**, *9*, 101–113.
- (22) Hook, A. L.; Voelcker, N. H.; Thissen, H. *Acta Biomater.* **2009**, *5*, 2350–2370.
- (23) Beebe, D. J.; Moore, J. S.; Bauer, J. M.; Yu, Q.; Liu, R. H.; Devadoss, C.; Jo, B. H. *Nature* **2000**, *404*, 588–590.
- (24) Hyun, J.; Lee, W. K.; Nath, N.; Chilkoti, A.; Zauscher, S. *J. Am. Chem. Soc.* **2004**, *126*, 7330–7335.
- (25) Plunkett, K. N.; Zhu, X.; Moore, J. S.; Leckband, D. E. *Langmuir* **2006**, *22*, 4259–4266.
- (26) Kaehr, B.; Shear, J. B. *Proc. Natl. Acad. Sci. U.S.A.* **2008**, *105*, 8850–8854.
- (27) Jonas, A. M.; Hu, Z.; Glinel, K.; Huck, W. T. S. *Nano Lett.* **2008**, *8*, 3819–3824.
- (28) Pokroy, B.; Epstein, A. K.; Persson-Gulda, M. C. M.; Aizenberg, J. *Adv. Mater.* **2009**, *21*, 463–469.
- (29) Pokroy, B.; Kang, S. H.; Mahadevan, L.; Aizenberg, J. *Science* **2009**, *323*, 237–240.
- (30) Shields, A. R.; Fiser, B. L.; Evans, B. A.; Falvo, M. R.; Washburn, S.; Superfine, R. *Proc. Natl. Acad. Sci. U.S.A.* **2010**, *107*, 15670–15675.
- (31) Yu, C.; Mutlu, S.; Selvaganapathy, P.; Mastrangelo, C. H.; Svec, F.; Frechet, J. M. J. *Anal. Chem.* **2003**, *75*, 1958–1961.
- (32) Pelah, A.; Jovin, T. M. *ChemPhysChem* **2007**, *8*, 1757–1760.
- (33) Na, K.; Jung, J.; Kim, O.; Lee, J.; Lee, T. G.; Park, Y. H.; Hyun, J. *Langmuir* **2008**, *24*, 4917–4923.
- (34) Hu, Z. B.; Chen, Y. Y.; Wang, C. J.; Zheng, Y. D.; Li, Y. *Nature* **1998**, *393*, 149–152.
- (35) Ionov, L.; Minko, S.; Stamm, M.; Gohy, J. F.; Jerome, R.; Scholl, A. J. *Am. Chem. Soc.* **2003**, *125*, 8302–8306.
- (36) Kim, H. S.; Crosby, A. J. *Adv. Mater.* **2011**, *23*, 4188–4192.
- (37) Kim, J.; Yoon, J.; Hayward, R. C. *Nat. Mater.* **2010**, *9*, 159–164.
- (38) Han, S.; Hagiwara, M.; Ishizone, T. *Macromolecules* **2003**, *36*, 8312–8319.
- (39) Ishizone, T.; Seki, A.; Hagiwara, M.; Han, S.; Yokoyama, H.; Oyane, A.; Deffieux, A.; Carlotti, S. *Macromolecules* **2008**, *41*, 2963–2967.
- (40) Lutz, J. F.; Hoth, A. *Macromolecules* **2006**, *39*, 893–896.
- (41) Jonas, A. M.; Glinel, K.; Oren, R.; Nysten, B.; Huck, W. T. S. *Macromolecules* **2007**, *40*, 4403–4405.
- (42) Laloyaux, X.; Fautré, E.; Blin, T.; Purohit, V.; Leprince, J.; Jouenne, T.; Jonas, A. M.; Glinel, K. *Adv. Mater.* **2010**, *22*, 5024–5028.
- (43) Christman, K. L.; Schopf, E.; Broyer, R. M.; Li, R. C.; Chen, Y.; Maynard, H. D. *J. Am. Chem. Soc.* **2009**, *131*, 521–527.
- (44) Krsko, P.; Sukhishvili, S.; Mansfield, M.; Clancy, R.; Libera, M. *Langmuir* **2003**, *19*, 5618–5625.
- (45) Sofia, S. J.; Merrill, E. W. *J. Biomed. Mater. Res.* **1998**, *40*, 153–163.
- (46) Tirumala, V. R.; Divan, R.; Ocola, L. E.; Mancini, D. C. *J. Vac. Sci. Technol., B* **2005**, *23*, 3124–3128.
- (47) Saaem, I.; Tian, J. *Adv. Mater.* **2007**, *19*, 4268–4271.
- (48) Kolodziej, C. M.; Maynard, H. D. *Chem. Mater.* **2012**, *24*, 774–780.